Simulation of capturing CO_2 from flue gas and syngas by pressure swing adsorption

CHENG-TUNG CHOU [1a], YU-JEN CHEN [1], CHIEN-SHUN CHANG [1], HONG-SUNG YANG [2], MING-WEI YANG [3], SSU-HUNG TU [3], ZONG-YU ZHUANG [3],
[1] Department of Chemical and Materials Engineering,
National Central University,
No. 300, Zhongda Rd., Zhongli District, Taoyuan City 32001
TAIWAN
[2] Department of Applied Cosmetology,
Hwa-Hsia University of Technology,
No. 111, Gongzhuan Rd., Zhonghe District, New Taipei City 235
TAIWAN
[3] Taipower Research Institute, Taiwan Power Company,
No.84, Da'an Rd., Shulin Dist., New Taipei City 238,
TAIWAN
[a] Email: t310030@ncu.edu.tw

Abstract: - Global warming is getting more serious in recent years. To reduce the emission of CO_2 is a major task nowadays. This research studies concentrating carbon dioxide from the flue gas of a power plant and from syngas after water gas shift reaction by pressure swing adsorption (PSA) process, so that the concentrated carbon dioxide can be captured to reduce the greenhouse effect. Zeolite 13X is used as adsorbent in this study. In the beginning of this study, the experimental adsorption isotherm data were regressed to obtain the parameters of Langmuir-Freundlich isotherm. Then the mass transfer coefficient of linear driving force (LDF) model were calculated by theory and verified by breakthrough curve experiments. At the end of this study, both dual-bed six-step PSA process for syngas (41.4% CO_2, 1.3% CO, 57.3% H_2) feed and three-bed twelve-step PSA process for flue gas (15%CO_2, 85%N_2) feed were studied to find the optimal operating conditions.

Key-Words: - pressure swing adsorption, simulation, carbon dioxide, 13X zeolite, flue gas, syngas

1 Introduction

Since Industrial Revolution in 19th century, the requirement of fossil fuels (coal, petroleum, natural gas, etc.) increases dramatically because of the rapid growth of economy. The large amount of greenhouse gases, especially CO_2, influences the climate change seriously. According to Emission Database for Global Atmospheric Research (EDGAR), CO_2 emission is highly as 33.4 billion ton in 2013 [1], which is 48% higher than twenty years ago, and the concentration in atmosphere is increasing from 280 ppm (before Industrial Revolution) to 400 ppm [2]. The raise of CO_2 concentration will increase the global temperature and the surface temperature of the ocean. The report of Intergovernmental Panel on Climate Change (IPCC) in 2014 mentioned that the raise of global temperature must be controlled within 2℃ relative to the level before industrialization. Thus, reducing and controlling the emission of CO_2 is a priority nowadays.

Carbon capture, utilization and storage (CCUS) is a technology that is considered more and more important in these years. This technology is to remove CO_2 from flue gas and atmosphere by utilizing or storing it to reach the target of IPCC safely and permanently. We can use CO_2 to produce soft drinks, extract as supercritical fluid and feed the microalgaes directly, or turn it into chemicals for indirect usage. With these utilizations above, we can not only reduce the amount of CO_2 in atmosphere, but also increase its economic value.

The system of capturing CO_2 can be divided into three categories by combustion type: pre-combustion capture, post-combustion capture and oxy-fuel combustion.

Pre-combustion capture, starting with coal gasification in a high temperature gasifier to synthesize syngas, in which the major compositions are hydrogen and carbon monoxide. Second, syngas

was sent into water gas shift (WGS) reactor with steam to generate carbon dioxide and hydrogen. Third, the outlet stream from WGS reactor was put into separation process to separate carbon dioxide and purify hydrogen. The high concentration hydrogen can be used for power generation or other usage by hydrogen storage technologies. Because pre-combustion capture cannot directly be inserted into existing power plant, it needs to be redesigned and carries high constructing and operating costs [3].

Post-combustion capture has running as pilot plant nowadays. This capture system has low equipment cost and can be directly inserted into the existing power plant without too much adjustment. The power plant can still work even when we stop the capture procedure. Flue gas has low CO_2 concentration, which also lower the capture efficiency [4].

Oxy-fuel combustion uses pure oxygen to burn the fuel. Though it can produce flue gas which carries high concentration of CO_2 (80-98%) and can be stored directly [5], but it needs to separate SO_2 from product otherwise it will corrode the equipment in the long run. Besides, the oxygen is produced by separation process, which carries high energy cost [6].

There are several techniques to prevent CO_2 from emission. Absorption is a traditional technique to capture CO_2 by the reaction of sorbent and CO_2. The operating cost of absorption is high because the high energy consumption of the regeneration of sorbent.

Membrane separation and pressure swing adsorption (PSA) have more and more potential in CO_2 capture nowadays. Membrane can separate CO_2 from others at high pressure. Easy to operate and low operating cost make this technique competitive.

Pressure swing adsorption uses cyclic pressure swing process to separate gas mixture, according to the difference of adsorption capacity of adsorbent due to different pressure. Due to low cost estimated taking US$31.8 per ton of CO_2 [7], easy operation and the progression of adsorbent, PSA is a highly potential technology.

In this study, two feed gases for CO_2 capture were discussed. One is flue gas, which is from power plant, and the other is syngas, which is from water gas shift reactor after gasifier. Then simulation is utilized to design PSA process with 13X zeolite adsorbent to achieve the purpose of capturing and concentrating carbon dioxide. Finally, operating variables are discussed to find the best operating conditions.

2 Model Description

2.1 Mathematical modelling

The PSA dynamic model is made up of several partial differential equations, the following assumptions are made:

1. Mass transfer resistance between gas phase and solid phase is considered; linear driving force model is used.
2. Using extended Langmuir-Freundlich equation to calculate the equilibrium adsorption amount of each gas component on the adsorbent.
3. Only axial concentration and temperature gradient are considered.
4. The ideal gas law is applied.
5. Non-isothermal system is assumed.
6. The pressure drop along the bed can be neglected due to large particle size, which is verified by Ergun equation.

The above assumptions are used in following equations:

Overall mass balance:

$$-\frac{\partial q}{\partial z}=\frac{\varepsilon A}{R}\frac{\partial (P/T)}{\partial t}+(1-\varepsilon)A\sum_{i=1}^{n}\frac{\partial n_i}{\partial t} \tag{1}$$

Mass balance for component i:

$$\frac{\partial}{\partial z}\left(\frac{\varepsilon AD_{ax,i}P}{RT}\frac{\partial y_i}{\partial z}\right)-\frac{\partial (y_i q)}{\partial z}=\frac{\varepsilon A}{R}\frac{\partial}{\partial t}\left(\frac{y_i P}{T}\right)+(1-\varepsilon)A\frac{\partial n_i}{\partial t} \tag{2}$$

Energy balance:

$$\left(A\bar{k}\right)\frac{\partial^2 T}{\partial z^2}-\frac{\partial}{\partial z}\left(\bar{C}_p qT\right)-\pi Dh\left(T-T_\infty\right)$$
$$=\frac{\varepsilon A}{R}\frac{\partial}{\partial t}\left(\bar{C}_p P\right)+\left(1-\varepsilon\right)A\sum_{i=1}^{n}\frac{\partial}{\partial t}\left[n_i\left(\tilde{C}_{pi}T-H_i\right)\right]+\left(1-\varepsilon\right)\rho_s\hat{C}_{ps}A\frac{\partial T}{\partial t} \tag{3}$$

Linear driving force model:

$$\frac{\partial n_i}{\partial \mathrm{t}}=k_{LDF,i}(n_i^*-n_i) \tag{4}$$

Boundary conditions can be assumed as [8]:

At inlet end:

$$y_i=y_{in,i}\ ,\ T=T_{in} \tag{5}$$

At outlet end:

$$\frac{\partial y_i}{\partial \mathrm{z}}=0\ ,\ \ \frac{\partial \mathrm{T}}{\partial \mathrm{z}}=0 \tag{6}$$

At two ends of the bed, the flow rate are estimated by using the valve equation recommended by Fluid Controls Institute, Inc. [9]:

$$Q^*=77.01c_v\left[\frac{P_1^2-P_2^2}{SG\times T}\right]^{1/2}\ ,\ \text{for } \mathrm{P_2} > 0.53\mathrm{P_1} \tag{7}$$

$$Q^*=65.31c_v P_1\left[\frac{1}{SG\times T}\right]^{1/2}\ ,\ \text{for } \mathrm{P_2} \le 0.53\mathrm{P_1} \tag{8}$$

Fifty-one basic grid points are marked in the bed to set up the initial concentration, temperature and pressure. The partial differential equations are converted to ordinary differential equations by method of lines. The spatial derivatives of

concentration, temperature, etc, are evaluated by central differences at every grid point. The cubic spline approximation is used to estimate the derivatives of flow rates and pressure with respect to time in the adsorption bed. The concentration, temperature and adsorption quantity in the bed are integrated in time by implicit Adams method in ODEPACK software with time step of 0.1s. The simulation is stopped when the system reaches cyclic steady state by using Eq. (9).

$$\sum\left(1-\frac{\text{Yi(last cycle)}}{\text{Yi(this cycle)}}\right)^2 < 1\times 10^{-4} \quad (9)$$

where Yi is the variable such as concentration, temperature, pressure, etc.

2.2 Adsorption isotherm on UOP 13X zeolite

In this study, UOP 13X zeolite is used to adsorb CO_2 from flue gas and syngas. The isotherm parameters of CO_2 and N_2 are regressed from measured adsorption data at different temperature. The adsorption data of H_2 and CO on 13X zeolite are from Delgado et al. [10], which are also regressed to obtain isotherm parameters. The model parameters of different gas adsorption on UOP 13X zeolite for Eq. (10) are listed in Table 1.

Langmuir-Freundlich isotherm for multiple components:

$$q_i^* = \frac{n_i^*}{\rho_s} = \frac{q_{m,i} b_i y_i^{m_i} P_j^{m_i}}{1+\sum_{j=1}^{n} b_i y_i^{m_i} P_j^{m_i}} \quad (10)$$

$$q_{m,i} = a_{i,1} + a_{i,2} T$$

$$b_i = b_{i,0} \exp\left(b_{i,1}/T\right)$$

$$m_i = m_{i,1} + m_{i,2}/T$$

Table 1. Values of model parameters in Eq. (10) for UOP 13X zeolite

	Carbon dioxide	Nitrogen	Carbon monoxide	Hydrogen
$a_{i,1}$ (mol/kg)	6.249	1.16×10^{2}	10.41	4.14
$a_{i,2}$ (mol /kg*K)	-4.20×10^{-3}	-1.28×10^{-1}	-2.68×10^{-2}	-6.24×10^{3}
$b_{i,0}$ (1/atm)	6.799×10^{-3}	1.652×10^{-4}	3.93×10^{-2}	1.21×10^{-4}
$b_{i,1}$ (K)	1.90×10^{3}	9.79×10^{2}	7.10×10^{2}	1.28×10^{3}
$m_{i,1}$ (-)	9.67×10^{-1}	1.12	2.15	1.54
$m_{i,2}$ (K)	-2.33×10^{1}	-1.39×10^{2}	-3.54×10^{2}	-1.55×10^{2}

2.3 PSA processes

In this study, two PSA process are discussed to capture CO_2 from different feed gases: syngas and flue gas.

For syngas, we simplified the composition to 41.4% CO_2, 1.3% CO and 57.3% H_2. The dual-bed six-step process shown as Fig.1 is utilized and the process is described as follows:

•Step 1, 6. Adsorption:

The adsorption bed is kept at high pressure by opening the valve 2 and feeding the gas consistently. At this time, most strong adsorptive gas (CO_2) adsorbs and weak adsorptive gas (H_2) exhausts from the top of bed.

•Step 2. Pressure equalization:

To equalize the pressures between two adsorption beds, valve 1 is closed and valve 3 is opened. The pressures of both beds become equal very soon.

•Step 3. Cocurrent depressurization:

In this step, valve 4 is opened to depressurize the adsorption bed. The major purpose of this step is to increase the concentration of strong adsorptive gas in gas phase.

•Step 4. Countercurrent depressurization (vacuum):

To vacuum the adsorption bed, valve 4 is closed and valve 5 is opened. The strong adsorptive gas desorbs from the solid phase due to the decrease of pressure which makes the concentration of strong adsorptive gas of gas phase increase, and exits from the bed.

•Step 5. Pressure equalization:

After step 4, the adsorption bed is at low pressure. To pressurize the bed in an efficient way, valve 3 is opened, the pressures of both bed become equal very soon.

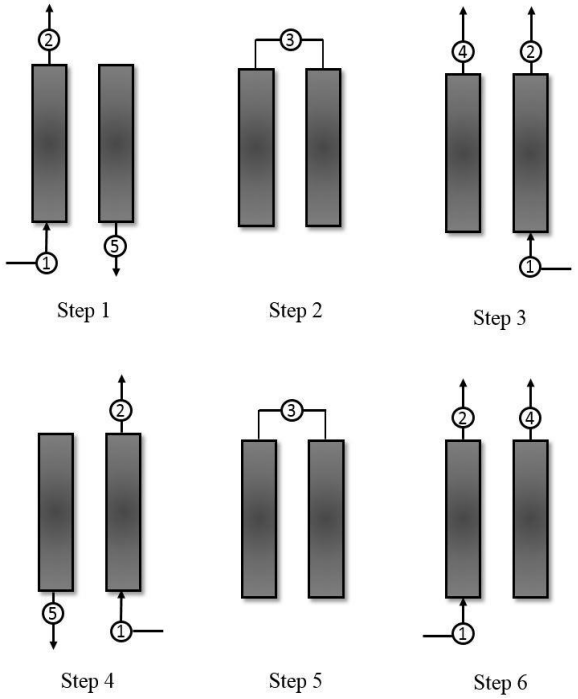

Fig.1. Schematic diagram of dual-bed six-step PSA process

The basic operating condition of dual -bed six-step PSA process is shown in Table 2.

Table 2.Basic operating condition of dual-bed six-step PSA process for syngas

Feed composition	41.4% CO_2, 1.3% CO, 57.3% H_2
Feed flow rate (L/min, STP)	4.6
Bed length (cm)	100
Bed inner diameter (cm)	2.32
Bed volume (L)	0.423
Bed prosity (-)	0.689
Fluid viscosity (g/cm-s)	1.67×10^{-4}
Density of fluid (g/cm^3)	2.45×10^{-3}
Feed temperature (K)	338.14
Surrounding temperature (K)	298.14
Feed pressure (atm)	3.45
Product pressure (atm)	1
Vacuum pressure (atm)	0.12
Step time (s)	90, 5, 10, 90, 5, 10

For flue gas, we simplifies the composition to 15% CO_2 and 75% N_2. The three-bed twelve-step process shown as Fig.2 is utilized and the process is described as follows:

•Step 1, 2, 12. Adsorption:
The adsorption bed is kept at high pressure by opening the valves 1 and 2, and feeding the gas consistently. At this time, most strong adsorptive gas (CO_2) adsorbs and weak adsorptive gas (N_2) exhausts from the top of bed.
•Step 3, 4. Pressure equalization:
The purpose is to equalize the pressures between two adsorption beds. At first pressure equalization, valve 1 is closed and valve 4 is opened. The pressures of both beds become equal very soon. Then valve 5 is opened to do second pressure equalization with bed 3.
•Step 5. Cocurrent depressurization:
In this step, valve 6 is opened to depressurize the adsorption bed. The major purpose of this step is to increase the concentration of strong adsorptive gas in gas phase.
•Step 6. Countercurrent depressurization (vacuum):
To vacuum the adsorption bed, valve 6 is closed and valve 3 is opened. The strong adsorptive gas desorbs from the solid phase due to the decrease of pressure which makes the concentration of strong adsorptive gas of gas phase increase, and exits from the bed.
Step 7, 9, 10. Idle
The valves of the inlet and outlet of the bed are closed.
•Step 8, 11. Pressure equalization:
This step is to pressurize the bed by other high pressure bed. The purpose of this step is to decrease the energy cost of feed pressurization by the above-mention method.

The basic operating condition of three-bed twelve-step PSA process is shown in Table 3.

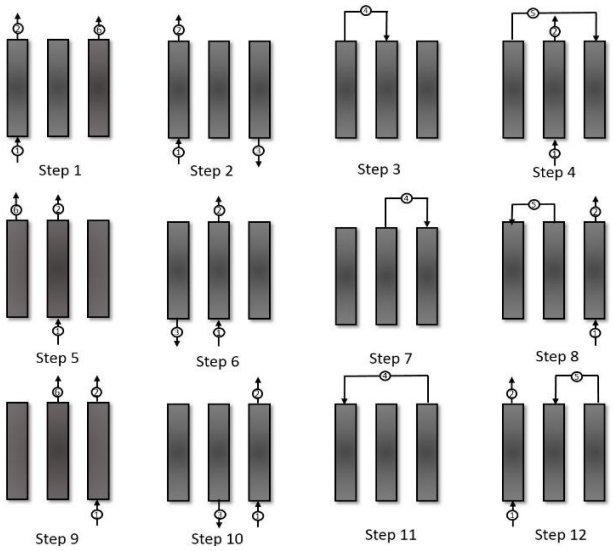

Fig.2. Schematic diagram of three-bed twelve-step PSA process

Table 3. Basic operating condition of three-bed twelve-step PSA process for flue gas

Feed composition	15% CO2, 85% N2
Feed flow rate (L/min, STP)	11.02*10^4
Bed length (cm)	600
Bed inner diameter (cm)	200
Bed volume (L)	18850
Bed prosity (-)	0.689
Fluid viscosity (g/cm-s)	1.87*10^-4
Density of fluid (g/cm^3)	2.59*10^-3
Feed temperature (K)	338.14
Surrounding temperature (K)	298.14
Feed pressure (atm)	2.37
Product pressure (atm)	1
Vacuum pressure (atm)	0.038
Step time (s)	60,120,30,30,60,120,30,30,60,120,30,30

3 Results and Discussion

3.1 Simulation verification

When the feed gas is fed into the bed constantly, as time goes on, the adsorbent becomes saturated and the concentration of outlet gas becomes as same as feed gas. This phenomenon is called breakthrough. The breakthrough curve equipment is shown in Fig.3. This experiment is used to verify the mass transfer coefficient ($k_{LDF,i}$) of linear driving force model predicted by theory [11]. The operating condition is shown in Table 4 and the results are shown in Fig.4. It shows that our simulation results are very close to the experimental data. Therefore, the accuracy of simulation program can be trusted.

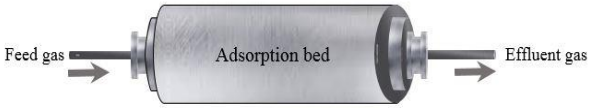

Fig.3. Schematic diagram of breakthrough curve experiment

Table 4. Operating parameters of breakthrough curve of gas mixture

Feed composition	15% CO_2, 85% N_2
Feed flow rate (L/min, STP)	100
Bed length (cm)	2.32
Bed diameter (cm)	0.423
Bed volume (L)	1.97
Feed pressure (atm)	298.14
Feed temperature (K)	298.14
Surrounding temperature (K)	1.53

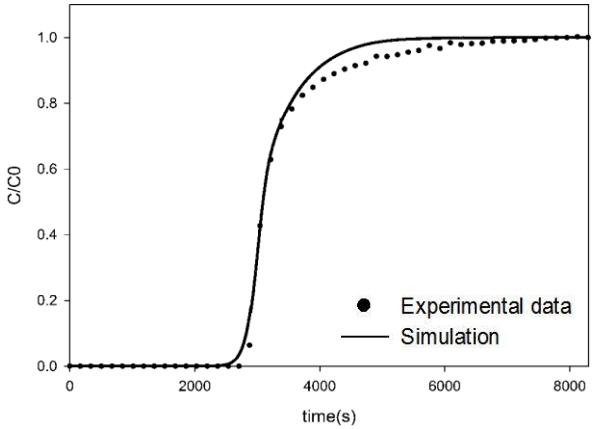

Fig.4. Breakthrough curve of CO_2 for gas mixture (15% CO_2, 85% N_2)

3.2 PSA process parameter study

3.2.1 Dual-bed six-step PSA process for syngas feed

To separate CO_2 and H_2 from syngas, dual-bed six-step PSA process is used. There are many operating variables to be discussed, such as bed length, feed flow rate, feed temperature, feed pressure, vacuum pressure, adsorption time and cocurrent depressurization time. The main simulation results are as following:

Effect of bed length

As bed length increases, the total adsorption amount of CO_2 on adsorbent increases, but the weak adsorpive gas remains occupied in the gas phase of bed, which makes the CO_2 recovery increase and purity decrease, shown in Fig.5.

Effect of feed flow rate

The total amount of feed gas increases while the feed flow rate increases. More weak adsorptive gas exits from the top, while the total adsorption capacity of adsorbent is fixed. It makes the purity of CO_2 increase but the CO_2 recovery decrease, shown in Fig.6.

Effect of feed temperature

The simulation results show that there is no significant influence on CO_2 in both purity and recovery when feed temperature increases from 298 K to 358 K.

Effect of feed pressure

The adsorption capacity of adsorbent increases with feed pressure increase. The simulation results show that the purity and recovery of CO_2 both increase as feed pressure increase, shown in Fig.7.

Effect of vacuum pressure

When vacuum pressure increases, more CO_2 becomes still adsorbed in the adsorbent during vacuum step, which makes the adsorbent regeneration not complete. However, simulation results show that there is only sligh influence on both CO_2 purity and recovery when vacuum pressure varies from 0.07 atm to 0.15 atm.

Effect of adsorption time

Here the adsorption time of step 1 is varied, but the adsorption time of step 6 is fixed to study the effect of adsorption time. The total amount of feed increases along with the adsorption time, and the adsorption time of step 1 is same as the countercurrent depressurization time of step 4 shown in Fig.1. Because more gas exits from the top, the CO_2 purity of bottom product increases but the recovery of CO_2 decrease as shown in Fig.8.

Effect of cocurrent depressurization time

The effet of cocurrent depressurization time is discussed in the section, but it also influences the adsorption time of step 6 at the same time, which is shown in Fig.1. The tendency of CO_2 purity and recovery change is same as the effect of adsorption time because of the similar reason.

Optimal condition

After all the variables are discussed, the optimal operating condition is adsorption bed length 100 cm, feed pressure 4.45 atm, feed temperature 338.14 K, vacuum pressure 0.09 atm, feed flow rate 4.6 L/min, STP, adsorption time 140 s, cocurrent depressurization time 10s, and countercurrent depressurization time 130 s. The simulation results show that the purity is 96.95% for CO_2 and 96.72% for H_2, and the recovery is 96.6% for CO_2 and 99.16% for H_2.

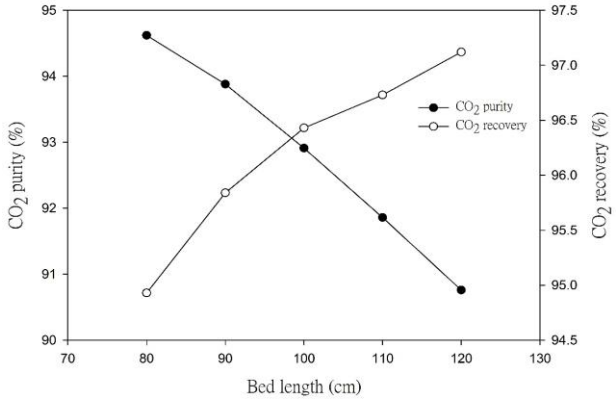

Fig.5. Effect of bed length on CO_2 purity and recovery in bottom product

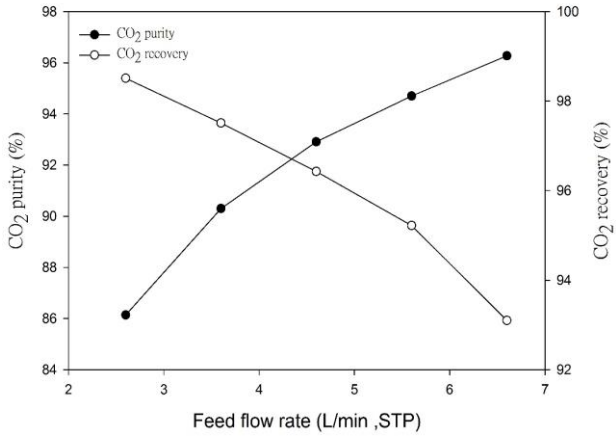

Fig.6. Effect of feed flow rate on CO_2 purity and recovery in bottom product

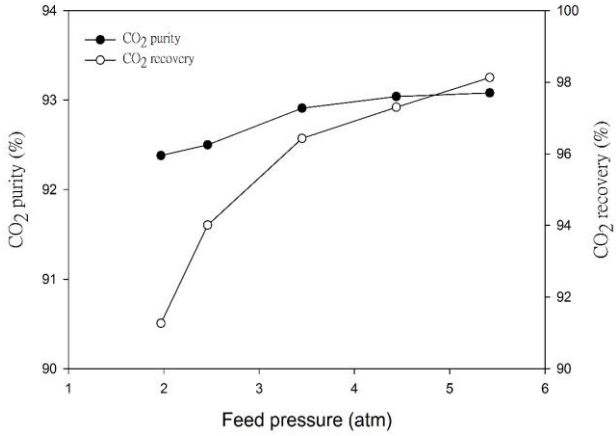

Fig.7. Effect of feed pressure on CO_2 purity and recovery in bottom product

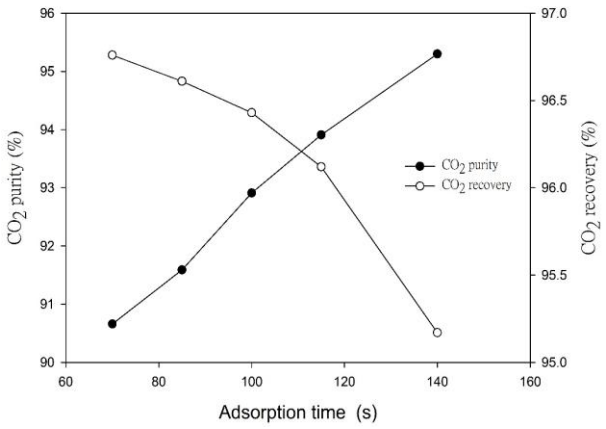

Fig.8. Effect of adsorption time on CO_2 purity and recovery in bottom product

3.2.1 Three-bed twelve-step PSA process

To separate CO_2 and N_2 from flue gas, three-bed twelve-step PSA process is used. There are many operating variables to be discussed, such as bed length, feed temperature, feed pressure, vacuum pressure, feed adsorption time and cocurrent depressurization time. The simulation results are as following:

Effect of bed length

As adsorption bed length increases, the amount of adsorbent increases so does the total adsorption capacity. The recovery of CO_2 increases, but the purity of CO_2 decreases as bed length increases, because the adsorption bed is too long for N_2 to exit. The simulation results are shown in Fig.9.

Effect of feed temperature

For UOP 13X zeolite, as the temperature increases, the selectivity of CO_2 increases, but the capacity decreases. These reasons cause that the purity of CO_2 increases but the CO_2 recovery decreases as feed temperature increases, as shown in Fig.10.

Effect of feed pressure

The pressure of adsorption bed increases while feed pressure increases, which makes the adsorption capacity of adsorbent increases. Fig.11 shows that the CO_2 recovery increases is due to the increases of adsorption capacity, but the purity of CO_2 decreases.

Effect of vacuum pressure

As vacuum pressure decreases, the regeneration of adsorbent becomes not complete. However the simulation results show that there is no significant influence on CO_2 in both purity and recovery when vacuum pressure increases from 0.03 atm to 0.05 atm.

Effect of adsorption time

The adsorption time is the sum of step times of steps 1, 2 and 12. By fixing the step time of steps 1 and 2, and varying the step time of step 12, we study the effect of adsorption time, as shown in Fig.2. When the time increases, the total amount of feed increases but the amount of adsorbate does not change. Fig.12 shows the recovery of CO_2 decrease is because that the adsorbent is saturated and part of CO_2 exits from the top.

Effect of cocurrent depressurization time

The cocurrent depressurization time means the step time of step 1/step 5/step 9 as shown in Fig.2. As CO_2 exits from top when the cocurrent depressurization time increase, there also exits more weak adsorptive gas. Fig.13 shows that the recovery of CO_2 decreases but the purity increases as cocurrent depressurization time increases.

Optimal condition

After all variables are discussed, the optimal operating condition is bed length 550 cm, feed pressure 2.27 atm, feed temperature 338.14 K, vacuum pressure 0.038 atm, feed flow rate 110200 L/min,STP, adsorption time 240 s, cocurrent depressurization time 60 s, countercurrent depressurization time 120 s. The simulation results show that the CO_2 product in the bottom can reach 92.79% purity and 90.04% recovery.

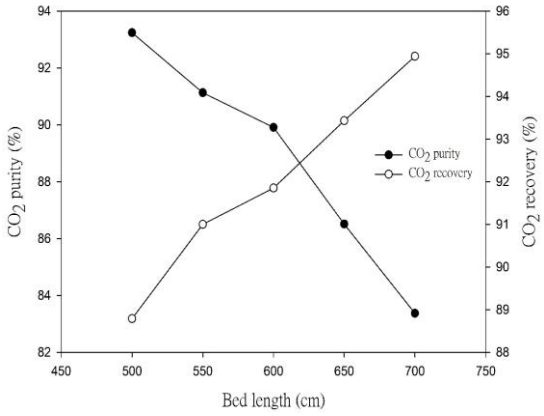

Fig.9. Effect of bed length on CO_2 purity and recovery in bottom product

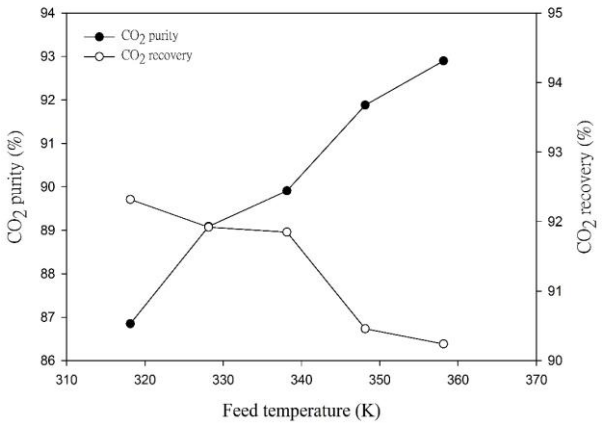

Fig.10. Effect of feed temperature on CO_2 purity and recovery in bottom product

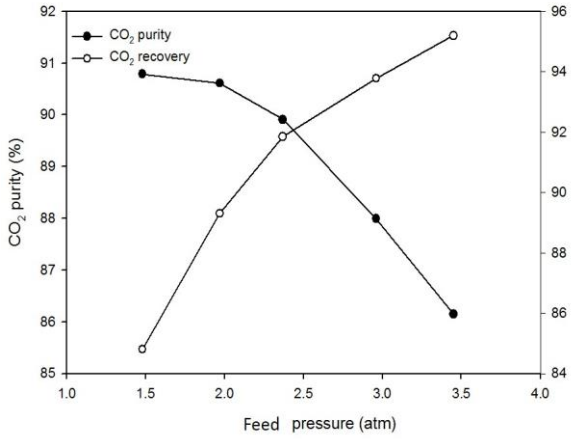

Fig.11. Effect of feed pressure on CO_2 purity and recovery in bottom product

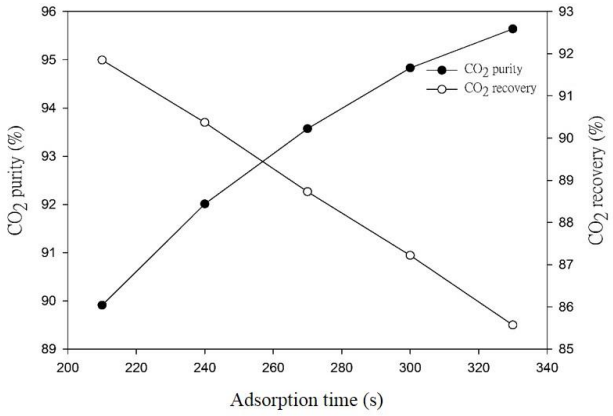

Fig.12. Effect of adsorption time on CO_2 purity and recovery in bottom product

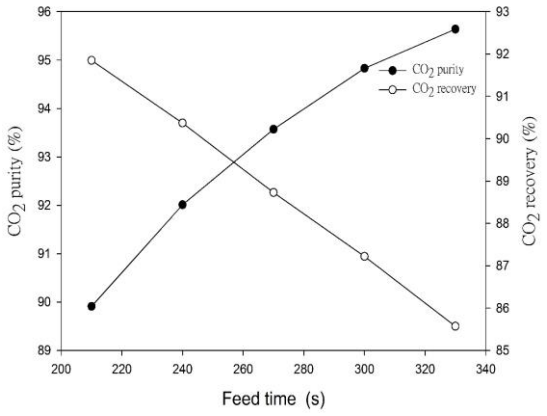

Fig.13. Effect of cocurrent depressurization time on CO_2 purity and recovery in bottom product

4 Conclusion

The purpose of this study is to reduce the CO_2 emission. Two PSA processes are utilized to separate CO_2 from flue gas and syngas with adsorbent 13X zeolite. After obtaining the isotherm parameters by regression from measured adsorption data and literature data, and the mass transfer coefficient k_{LDF} of linear driving froce model from theroy, the verification of simulation program was accomplished. The results from the experimental breakthrough curve data show the reliability of simulation program. To separate CO_2 from different gas sources, two PSA processes are used: dual-bed six-step PSA process for syngas feed and three-bed twelve-step for flue gas feed. After the discussion of operating variables, the results show that for syngas feed, the dual-bed six-step PSA process utilized gives a CO_2 product in the bottom with 96.95% CO_2 purity and 96.6% CO_2 recovery, and a H_2 top stream with 96.72% H_2 purity and 99.16% H_2 recovery. For flue gas feed, the three-bed twelve-step PSA process utilized produces CO_2 product in the bottom reaching 92.79% purity and 90.04% recovery. We provide two possible processes to decrease the amount of CO_2 exhausted to atmosphere. Hoping to reduce the energy consumption and construct the PSA apparatus, making the reduction of CO_2 into reality.

Nomenclature

A sectional area of adsorption bed [cm^2]
$\widetilde{C}_{pi}$ heat capacity of component i [J/mol-K]
$\widehat{C}_{ps}$ heat capacity of solid phase [J/g-K]
$\overline{C}_P$ average heat capacity of gas phase [J/mol-K]
c_v valve coefficient [-]
D diameter of adsorption bed [cm]
$D_{ax,i}$ axial dispersion coefficient of component i [cm^2/s]
h heat transfer coefficient [J/K-cm^2-s]
H_i adsorption heat of component i [J/mol]
$k_{LDF,i}$ mass transfer coefficient of linear driving force model of component i [1/s]
$\overline{k}$ average thermal conductivity [J/K-cm-s]
n number of gas component
n_i adsorption amount of component i per unit volume of adsorbent [mol/cm^3]
n_i^* equilibrium adsorption amount of component i per unit volume of adsorbent [mole/cm^3]
P pressure [atm]
P_1 inlet pressure of valve [atm]
P_2 outlet pressure of valve [atm]
Q^* flow rate at standard temperature and pressure [L/s, STP]
q molar flow rate [mol/s]
q_i^* equilibrium adsorption amount of component i per unit mass of adsorbent [mole/g]
$q_{m,i}$ saturated adsorption amount of component i per unit mass of adsorbent [mole/g]
R gas constant [82.057 atm-cm^3/mol-K]
SG specific gravity of gas [-]
T temperature [K]
T_{in} temperature of inlet gas [K]
T_∞ surrounding temperature [K]
Yi the variable of concentration, temperature, pressure, etc.
y_i molar fraction of component i in gas phase [-]
$y_{in,i}$ molar fraction of component i in inlet gas [-]
z position in the adsorption bed [cm]

Greek symbols

ε voidage of adsorption bed [-]
ρ_s particle density of adsorbent [g/cm^3]

Acknowledgement

The authors gratefully acknowledge the financial support of the NEP-II program of Ministry of Science and Technology, Taiwan under project number MOST 105-3113-E-008-001, and the project of Taiwan Power Research Institute, Taiwan Power Company under contract number 5460400010 and 5460500083.

References:

[1] Emission database for global atmospheric research EDGAR , European Commission, European Commission. Report available on: http://edgar.jrc.ec.europa.eu/overview.php?

[2] R.K. Pachauri and L.A. Meyer, Climate Change 2014: Synthesis Report, IPCC, Geneva, 2014.

[3] E. Rubin and H. de Coninck, IPCC special report on carbon, Cambridge University, UK, 2004.

[4] ICF International, Developing a pipeline infrastructure for CO2 capture and storage: issues and challenges, Technical report prepared for INGAA Foundation., 2009.

[5] Zero Emissions Resource Organization, 2013. Report available on: http://www.zeroCO2.no.

[6] I. Pfaff and A. Kather, Comparative thermodynamic analysis and integration issues of CCS steam power plants based on oxy-combustion with cryogenic or membrane based air separation, *Emergu Procedia*, Vol.1, 2009, pp. 495-502.

[7] N. Susarla, R. Haghpanah, I.A. Karimi, S. Farooq, A. Rajendran, L.S.C. Tan, J.S.T. Lim, Energy and cost estimates for capturing CO_2 from a dry flue gas using pressure/vacuum swing adsorption, *Chemical Engineering Research and Design*, Vol.102, 2015, pp. 354-367.

[8] P. V. Danckwerts, Continuous flow systems: Distribution of residence, *Chemical Engineering Science*, Vol.2, 1953, pp. 1–13.

[9] C.T. Chou and C.Y. Chen, Carbon Dioxide Recovery by Vacuum Swing Adsorption, *Separation and Purification Technology*, Vol. 39, No. 1-2, 2004, pp. 51-65

[10] J. A. Delgado, V. I. Águeda, M. A. Uguina, J. L. Sotelo, P. Brea, and C. A. Grande, Adsorption and Diffusion of H2, CO, CH4, and CO2 in BPL Activated Carbon and 13X Zeolite: Evaluation of Performance in Pressure Swing Adsorption Hydrogen Purification by Simulation, *Ind. Eng. Chem. Res*, Vol.10, 2014, pp. 15414-15426.

[11] S. Ruthven and D.M. Farooq, Heat effects in adsorptioncolumn dynamics. 2. Experimental validation of theone-dimensional model, *Ind. Eng. Chem. Res.*, Vol.29, 1990, pp. 1084-1090.